JOURNAL OF NEUROPHYSIOLOGY
Vol. 68, No. 4, October 1992. *Printed in U.S.A.*

Physiological Properties of Primate Lumbar Motoneurons

JONATHAN S. CARP
Wadsworth Center for Laboratories and Research, New York State Department of Health, Albany, New York 12201-0509

SUMMARY AND CONCLUSIONS

1. Intracellular recordings were obtained from 149 motoneurons innervating triceps surae (n = 109) and more distal muscles (n = 40) in 14 pentobarbital-anesthetized monkeys (*Macaca nemestrina*). The variables evaluated were resting membrane potential, action potential amplitude, conduction velocity (CV), input resistance (R_N), membrane time constant (τ_m), electrotonic length (L), whole-cell capacitance (C_{tot}), long current pulse threshold (rheobase), short current pulse threshold (I_{short}), afterhyperpolarization (AHP) maximum amplitude (AHP_{max}), AHP duration (AHP_{dur}), time to half maximum AHP amplitude ($AHP_{t½}$), depolarization from resting potential to elicit action potential (V_{dep}), and threshold voltage for action potential discharge (V_{thr}).

2. Mean values ± SD for the entire sample of motoneurons are as follows: resting membrane potential −67 ± 6 mV; action potential amplitude 75 ± 7 mV; CV 71 ± 6 m/s; R_N 1.0 ± 0.5 MΩ; τ_m 4.4 ± 1.5 ms; L 1.4 ± 0.2 λ; C_{tot} 7.1 ± 1.8 nF; rheobase 13 ± 7 nA; I_{short} 29 ± 14 nA; AHP_{max} 3.5 ± 1.3 mV; AHP_{dur} 77 ± 26 ms; $AHP_{t½}$ 21 ± 7 ms; V_{dep} 11 ± 4 mV; and V_{thr} −56 ± 5 mV. CV is lower in soleus than in either medial or lateral gastrocnemius motoneurons, and R_N is lower and τ_m is longer in soleus than in lateral gastrocnemius motoneurons.

3. R_N is higher in motoneurons with longer τ_m and slower CV. A linear relationship exists between log(CV) and log($1/R_N$) with a slope of 1.8–2.2 (depending on the action potential amplitude acceptance criteria used), suggesting that membrane resistivity (R_m) does not vary systematically with cell size.

4. Rheobase is higher in motoneurons with lower R_N, longer τ_m, shorter AHP time course, and higher CV. I_{short} and normalized rheobase (i.e., rheobase/C_{tot}) vary similarly with these motoneuron properties, except that I_{short} is independent of τ_m and normalized rheobase is independent of CV.

5. V_{thr} tends to be more depolarized in motoneurons with large C_{tot}, but the relationship is sufficiently weak so that any systematic variation in V_{thr} according to cell size probably contributes only minimally to recruitment order. V_{thr} does not vary systematically with CV, AHP time course, R_N, or τ_m.

6. Quantitative differences between macaque and cat triceps surae motoneurons are apparent in CV, which is slower in macaque than in cat, and to a lesser extent in τ_m and R_N, which are lower in macaque than in cat. These data, along with available anatomic data, suggest that R_m may be lower in macaque motoneurons than in cat motoneurons.

7. Comparison of the present primate data with those from cat suggests that intraspecies relationships between motoneuron properties are qualitatively similar. However, excitability of macaque motoneurons appears to vary systematically with motoneuron properties related to both R_m and cell size.

INTRODUCTION

Electrophysiological analyses of motoneurons and their synaptic inputs have furnished considerable insight into the organization of segmental motor output and have generated hypotheses accounting for the orderly recruitment of the motoneuron pool. However, almost all of these studies are in the cat or in other subprimate species. Few studies have provided data from nonhuman primates on the properties of motoneurons and their segmental synaptic interactions (Clough et al. 1968a; Hongo et al. 1984), and human data are currently limited to measurements of axonal conduction velocity (CV) (Smorto and Basmajian 1979) and indirect estimates of synaptic interactions (Ashby and Zilm 1982; Bergmans et al. 1978; Mao et al. 1984; Pierrot-Deseilligny et al. 1981). As a result, present models of motoneuron function and segmental motor organization are based largely on subprimate data, and their relevance to primates, including humans, is unclear. Further study of motoneuron properties in primates is essential.

The purpose of the experiments described here was to delineate the electrophysiological properties of spinal motoneurons innervating hind limb muscles, including triceps surae (TS) in monkey. The results permit comparison of primate with subprimate species and also serve as a control group for other primate studies now under way in this laboratory (Wolpaw 1987; Wolpaw and Lee 1989). Portions of this work have been presented in abstract form (Carp and Wolpaw 1990; Carp et al. 1989).

METHODS

Animal preparation

Experiments were performed in 14 male pigtail macaques (*Macaca nemestrina*) weighing between 4.5 and 9.3 kg (mean 7.1 kg). All animal procedures were in accord with DHEW Publication (NIH) 85-23, "Guide for the Care and Use of Laboratory Animals," and had been reviewed and approved by the Institutional Animal Care and Use Committee of the Wadsworth Center.

Anesthesia was induced with ketamine (7 mg/kg im) and then deepened and maintained with pentobarbital sodium (initial dose of 15 mg/kg iv, then 3–4 mg/kg iv every 30 min). A single dose of atropine was also administered at the time of induction (0.03 mg/kg im). An endotracheal tube was inserted to maintain airway patency, and the brachial vein was cannulated for drug administration and fluid replacement. Animals were supported in a rigid frame by stereotaxic headholder, hip pins, and clamps on the T_{11} spinous process and both knees. Throughout the experiment, heart rate, expired CO_2, and urine volume, specific gravity, and pH were monitored, and deep surgical anesthesia [verified regularly by absence of response to vigorous palpebral or tracheal stimulation; no respiratory or cardiac response to surgery (Green 1979; Steffey 1983)] was maintained. At the end of the study, the anesthetized animal was killed with an overdose of intravenous pentobarbital.

Following an L_1–L_6 dorsal laminectomy, the dura was cut longitudinally, gently retracted laterally, and pinned to the underlying

muscle. The dentate ligaments were cut, and the L_5–L_7 spinal cord segments were elevated ~4 mm above the vertebral column on a plastic platform. Lifting the spinal cord in this manner decreased movement artifacts caused by respiratory and cardiac pulsations and thus facilitated intracellular recording. The nerves innervating the TS muscles [i.e., medial gastrocnemius (MG), lateral gastrocnemius (LG), and soleus (SOL)] and the tibial nerve distal to the TS nerves (DT) were dissected free from surrounding tissue in both hind limbs, cut distally, and placed on bipolar stimulating electrodes. A silver monopolar electrode recorded the cord dorsum potential evoked by peripheral nerve stimulation. Mineral oil pools were formed by retracting the cut skin edges of the incisions in the back and legs. Heat lamps maintained the back mineral oil pool and rectal temperatures at 37–39°C and the leg mineral oil pools at 35–37°C.

Just before the beginning of the recording session, a bilateral pneumothorax was performed and the animal was ventilated with a respirator using room air. Neuromuscular blockade was then established with gallamine triethiodide (3 mg/kg iv initially, subsequently supplemented by 1.5 $mg \cdot kg^{-1} \cdot 30\ min^{-1}$). Because neuromuscular blockade prevented assessment of motor response to painful stimulation, maintenance of deep surgical anesthesia was ensured by continuing the established pentobarbital dosage schedule and by monitoring heart rate and pupillary light reflex. On the few occasions when heart rate increased or a pupillary light reflex was observed, the pentobarbital dosage was increased. Respiratory rate and volume were adjusted to maintain expired CO_2 at or slightly below prepneumothorax levels (typically 29–33 mmHg). In the last 10 experiments, dexamethasone (0.25 $mg \cdot kg^{-1} \cdot h^{-1}$ iv) was begun at the time of the pneumothorax to reduce spinal cord edema over the 18- to 24-h period of intracellular study. Because no significant differences were found in any of the motoneuron properties described below between dexamethasone-treated and untreated animals, the data from all of these animals were treated as a single group.

Intracellular recording

Intracellular recordings from spinal motoneurons were performed with glass micropipettes initially formed with a vertical puller and then either beveled or reshaped using a microforge (Dold and Burke 1972). Electrodes were filled with 3 M potassium acetate plus 0.01 M KCl and had DC resistances of 2–8 MΩ. The micropipette tip was positioned between midline and the dorsal root entry zone of the L_6–L_7 segments with the electrode pointing laterally 15–25° from the vertical. The motoneuron pools were located by advancing the micropipette with a stepping microdrive through the spinal cord, seeking the extracellularly recorded antidromic field potential elicited by electrical stimulation of the peripheral nerves (2-Hz, 0.05-ms pulses from an isolated stimulator). Cells were recorded from both sides of the spinal cord. The micropipette was connected to a high-impedance amplifier. Bridge balance and capacitance compensation were adjusted for each cell to minimize the effects of electrode resistance and capacitance on the voltage recording. Membrane potential and a voltage signal proportional to injected current were low-pass filtered (DC-6 kHz) and amplified to take advantage of the full range of the analog-to-digital converter during sampling (≥12 kHz) by computer.

Criteria for inclusion in the data pool

Action potential amplitude is thought to be sensitive to impalement-induced damage. Thus it is commonly used as a criterion for acceptance of a cell into the data pool. However, there is little agreement on the most appropriate cutoff value to use. Data were obtained from 169 motoneurons with action potential amplitudes ranging from 47 to 92 mV. To select an appropriate value, input resistance (R_N) and membrane time constant (τ_m)—properties that would be expected to be sensitive to this type of damage (Jack 1979; Rose and Vanner 1988)—were compared in motoneurons grouped according to action potential amplitude (see *Electrophysiological properties* below for methodology). As Table 1 indicates, R_N and τ_m vary little with action potential amplitude for cells with action potentials ≥60 mV, but are low if action potentials are <60 mV. R_N and τ_m are slightly higher in cells with action potentials ≥80 mV than in those with action potentials ≥60 mV and <80 mV. On the basis of these data, only motoneurons with antidromically or current-evoked (0.5 ms pulse duration) action potentials of ≥60 mV and with stable resting membrane potentials are included in the data analysis presented here. The suitability of this cutoff value is supported by the lack of any statistically significant linear relationship between either resting potential and R_N or τ_m ($r^2 = 0.01$, $P > 0.2$ in both cases) for cells in the accepted range. The 60 mV cutoff is comparable to that used in some studies (Fleshman et al. 1981; Kernell and Zwaagstra 1981) but lower than that used in others (Gustafsson and Pinter 1984a,b). Given the more inclusive action potential amplitude cutoff used here, cases in which raising this cutoff affected statistical analysis are mentioned in the text.

Electrophysiological properties

In each motoneuron, a complete set of measurements of CV, current and voltage thresholds, R_N, time constants, and afterhyperpolarization (AHP) characteristics was attempted, but it was not always obtained because loss of resting membrane potential or decrease in action potential amplitude sometimes curtailed recording. In some cells, composite homonymous and heteronymous excitatory postsynaptic potentials (EPSPs) to peripheral nerve stimulation were recorded, but these data are not reported here.

CV was calculated as the distance between the proximal peripheral nerve stimulating electrode (cathode) and the intracellular recording site (measured postmortem after exposing the nerve) divided by the latency of the antidromic action potential. Because dorsal roots were left intact for EPSP recording, detection of anti-

TABLE 1. *Comparison of motoneuron properties among cells with different AP amplitudes*

	AP < 60 mV	60 mV ≤ AP < 70 mV	70 mV ≤ AP < 75 mV	75 mV ≤ AP < 80 mV	AP ≥ 80 mV
Membrane potential, mV*	−54 ± 8 (20)	62 ± 4 (36)	−65 ± 4 (35)	−68 ± 4 (48)	−72 ± 6 (30)
AP amplitude, mV*	55 ± 4 (20)	66 ± 3 (36)	73 ± 1 (35)	78 ± 2 (48)	84 ± 3 (30)
CV, m/s	71 ± 6 (20)	72 ± 5 (36)	72 ± 7 (35)	71 ± 5 (48)	68 ± 8 (30)
R_N, MΩ†	0.6 ± 0.3 (12)	1.0 ± 0.4 (30)	0.9 ± 0.4 (26)	0.9 ± 0.4 (44)	1.2 ± 0.6 (28)
τ_m, ms‡	2.6 ± 1.9 (11)	4.3 ± 1.7 (24)	4.1 ± 1.2 (23)	4.3 ± 1.1 (42)	4.8 ± 2.0 (28)

Values are means ± SD. Values in parentheses are number of cells. AP, action potential; CV, conduction velocity; R_N, input resistance; τ_m, membrane time constant. *$P < 0.001$ for overall difference among means. †$P < 0.01$ for overall difference among means; AP < 60 group significantly different from AP ≥ 80 group ($P < 0.01$). ‡AP < 60 group significantly different from 60 ≤ AP < 70, 75 ≤ AP < 80, and AP ≥ 80 groups ($P < 0.01$).

dromic firing and determination of latency was often difficult because of the presence of EPSPs of shorter latency, a problem that has also been reported in some cat motoneurons (Eccles et al. 1957). In such cases, responses with and without action potentials to a just-threshold stimulus were averaged (~25 responses each) and subsequently subtracted. The resulting trace provided an estimate of the antidromic action potential alone that was used for calculating the CV.

The AHP after an action potential was delineated by averages of 50 action potentials elicited by short (0.5 ms) current pulses. It was quantified in terms of three variables: *1*) maximum amplitude (AHP_{max}), defined as the difference between the resting potential and the most negative membrane potential observed during the AHP; *2*) duration (AHP_{dur}), defined as the time between the end of the action potential (i.e., when the membrane potential repolarized to the mean prespike resting potential) and membrane potential depolarization to within 2 SD of the mean prespike mean resting potential; and *3*) time to half amplitude ($AHP_{t½}$), defined as the difference between the time of occurrence of the AHP_{max} and the time when the AHP amplitude decreased to half of the AHP_{max}.

R_N and time constants were determined from averages of 75–125 voltage responses to two to six different small-amplitude (0.5–3.0 nA) 100-ms hyperpolarizing current pulses. R_N was estimated as the ratio of the maximal membrane potential deflection during the current pulse to the amplitude of the current pulse. Time constants were estimated from the membrane potential trajectory after the current pulse using a curve peeling method based on that described by Zengel et al. (1975). This method is based on a simple electrical model of the motoneuron (Ito and Oshima 1965) in which the voltage response is the sum of three first-order processes reflecting somatic (and proximal dendritic) passive current flow (τ_m), current redistribution between soma and dendrites (τ_{eq}), and activation of a conductance mechanism underlying a slower "sag" of the membrane potential back toward its resting level (τ_{sag}). The method for determining the time constants of these three processes is illustrated in Fig. 1. The procedure for determining R_N and time constants was performed as soon as the membrane potential and action potential amplitude stabilized. When possible, this procedure was repeated at the end of the cell's recording session. Final estimates of R_N and time constants were averages of all the individual values. Electrotonic length (L) was calculated on the basis of Rall's model of neuronal electrotonic behavior for sealed-end boundary conditions (Rall 1969) using estimates of τ_m and τ_{eq} obtained from the curve peeling procedure described above. Whole cell capacitance (C_{tot}) was estimated for motoneurons in which calculations of R_N, τ_m, and L were available using the equation described by Gustafsson and Pinter (1984a).

The sag phenomenon was present in almost all motoneurons studied, which could result in underestimation of R_N (Gustafsson and Pinter 1984a). The percent underestimation of R_N ($\%R_{err}$) was calculated from the fitted time constants and scaling factors obtained from the curve peeling procedure described above, where $\%R_{err}$ is defined as $\{[1 - (R_{N\ predicted\ by\ all\ three\ components}/R_{N\ predicted\ without\ sag\ component})] \times 100\}$ at the time when membrane potential reached its minimum. $\%R_{err}$ for the entire sample of motoneurons is 13 ± 5%, mean ± SD (range 3–27%). Values of R_N reported here are not corrected for error introduced by sag, because there is no systematic variation in $\%R_{err}$ among the four motoneuron pools (15 ± 6, 13 ± 4, 13 ± 5, and 13 ± 6% for MG, LG, SOL, and DT motoneurons, respectively) and there is no relationship between $\%R_{err}$ and R_N ($r^2 = 0.02$, $P > 0.1$ for linear regression). On the other hand, AHP_{dur} tended to be shorter in cells with higher $\%R_{err}$ ($r^2 = 0.15$, $P < 0.001$ for linear regression), which is consistent with observations in cat motoneurons (Gustafsson and Pinter 1984a) and the hypothesis that AHP time course is influenced by sag (Gustafsson and Pinter 1985b).

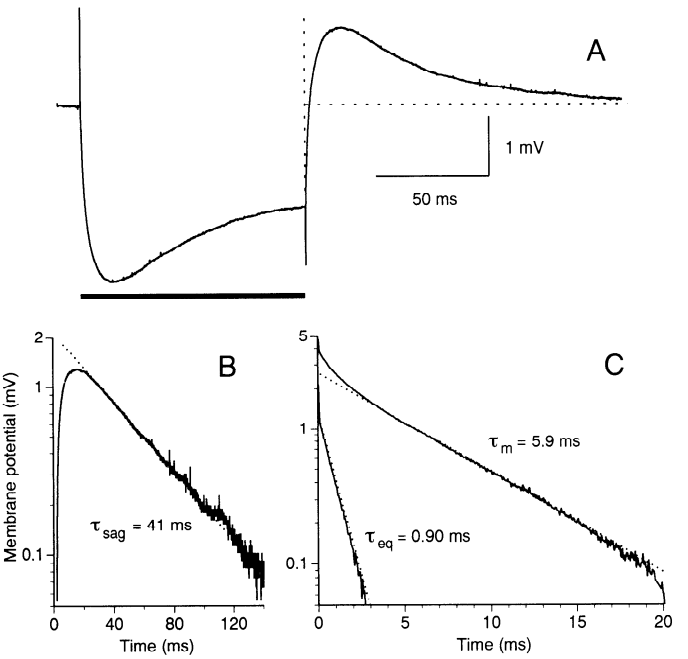

FIG. 1. Example of method of determining time constants from membrane potential trajectory in response to a 100-ms hyperpolarizing current pulse whose duration is indicated by the horizontal bar under the voltage trace (*A*). Membrane potential after the end of the current pulse is plotted as a function of time on semilogarithmic axes (*B* and *C*), where t = 0 corresponds to the end of the current pulse. Time constants are estimated as −1/slope of the regression line calculated over the linear portion of the voltage decay. After calculating the time constant for activation of a conductance mechanism underlying a slower sag of the membrane potential back toward its resting level [τ_{sag} (*B*)], the regression line is subtracted from the data, which is then replotted to allow calculation of the time constant for somatic and proximal dendritic passive current flow [τ_m (*C, top*)]. The process is then repeated to calculate the time constant for current redistribution between soma and dendrites [τ_{eq} (*C, bottom*)].

To determine long current pulse threshold (rheobase), short current pulse threshold (I_{short}), and action potential threshold, single action potentials were elicited by injection of long (100 ms) or short (0.5 ms) depolarizing current pulses that elicited an action potential in ~50% of the trials. Rheobase and I_{short} were defined as the amplitude of the long and short current pulses, respectively. The amount of depolarization from the resting potential required for action potential initiation (V_{dep}) was calculated as the difference between the action potential amplitude elicited by the short current pulse and that elicited by the long current pulse. The absolute threshold voltage for action potential initiation (V_{thr}) was calculated as the sum of the resting potential and V_{dep}. Because of the dependence of action potential amplitude on resting membrane potential (slope −0.72, $r^2 = 0.40$, $P < 0.0001$ for linear regression), V_{dep} and V_{thr} were calculated only for cells in which the difference in resting potential between long and short current pulse trials was ≤1 mV.

Statistical analysis

Statistical analysis of intergroup differences was performed using analysis of variance. Relationships between variables were assessed by linear regression. Differences with P values <0.01 were considered to be statistically significant. This stringent P value was considered appropriate given the large number of relationships evaluated.

RESULTS

Description of data pool

Data were obtained from 149 motoneurons with action potentials ≥60 mV and stable resting potentials. The sample consisted of 109 TS motoneurons (32 MG, 38 LG, and 39 SOL) and 40 DT motoneurons. Table 2 is a summary of the data from the entire sample of motoneurons, from TS motoneurons, and from each individual pool of motoneurons. There are significant differences among the individual motoneuron pools in CV, R_N, and τ_m ($P < 0.01$ for R_N, $P < 0.001$ for CV and τ_m by analysis of variance). Intergroup comparisons indicate that SOL motoneurons have slower CV than MG or LG motoneurons and have higher R_N and longer τ_m than LG motoneurons. DT motoneurons have slower CV and lower τ_m than MG motoneurons and lower R_N than SOL motoneurons. Rheobase tends to be lower in SOL than in the other motoneurons, but the difference does not meet the criterion for statistical significance used here ($0.04 > P > 0.03$). Values for all other motoneuron properties are similar among the four individual motoneuron pools.

It should be noted that some properties were measured in most motoneurons (e.g., R_N, τ_m, and L), whereas others were obtained from a more limited number (e.g., V_{dep}, V_{thr}, and AHP characteristics). Assessment of the latter properties often necessitated passing large currents intracellularly. Under this condition, nonlinear behavior of the electrodes sometimes rendered these measurements unreliable. In addition, threshold measurements were based on the results of two independent tests with a stringent criterion for matching resting potential between them, and thus were obtained from only about half of the cells.

There are no explicit electrophysiological criteria (e.g., CV ranges) in this species for determining whether these cells are α- or γ-motoneurons. However, EPSPs of monosynaptic latency were elicited in all motoneurons in which they were sought, including those with CVs as low as 54 m/s [monosynaptic EPSPs were not evaluated in the only 2 cells with lower CVs (49 and 52 m/s)]. Because γ-motoneurons in other species do not receive monosynaptic inputs (Baldissera et al. 1981), the present cell population probably consists predominantly, if not exclusively, of α-motoneurons.

In presenting the data, motoneurons are pooled from left ($n = 63$) and right ($n = 86$) sides of the spinal cord. This appears to be justified, because no statistically significant right/left differences are found for any of the variables tested in the entire population of motoneurons or for TS motoneurons alone ($P > 0.1$ for all comparisons).

The possibility that properties of motoneurons recorded early in the 18- to 24-h recording sessions were not equivalent to those recorded late (i.e., when the spinal cord was presumably less healthy because of prolonged deep anesthesia and multiple electrode penetrations) required evaluation. Resting potential and action potential amplitude did not appear to vary systematically over the prolonged time course of these experiments ($r^2 = 0.00$, $P > 0.4$ for linear regressions of membrane potential and action potential amplitude on time of recording). Thus pooling data from motoneurons studied throughout this time course appears to be justified.

The following sections assess the entire population of motoneurons and describe several relationships among their properties. Comparable relationships are also found for TS motoneurons alone.

Relationship between R_N and other motoneuron properties

Theoretically, R_N is expected to be determined by cell surface area, membrane resistivity (R_m), and cell geometry (Rall 1977). Data from cat motoneurons are generally consistent with this model (Burke et al. 1982; Fleshman et al. 1981; Gustafsson and Pinter 1984a). These relationships are evaluated below for macaque motoneurons.

TABLE 2. *Summary of macaque motoneuron properties*

	All cells	All TS	MG	LG	SOL	DT
Resting potential, mV	−67 ± 6 (149)	−66 ± 6 (109)	−65 ± 5 (32)	−67 ± 5 (38)	−66 ± 7 (39)	−68 ± 6 (40)
AP amplitude, mV	75 ± 7 (149)	75 ± 7 (109)	76 ± 7 (32)	74 ± 6 (38)	75 ± 7 (39)	75 ± 6 (40)
CV, m/s	71 ± 6 (149)	71 ± 7 (109)	74 ± 8 (32)	72 ± 5 (38)	68 ± 6 (39)	69 ± 5 (40)
R_N, MΩ	1.0 ± 0.5 (128)	1.0 ± 0.5 (94)	1.0 ± 0.5 (27)	0.8 ± 0.3 (32)	1.2 ± 0.5 (35)	0.9 ± 0.4 (34)
τ_m, ms	4.4 ± 1.5 (117)	4.6 ± 1.6 (84)	4.9 ± 1.6 (22)	3.9 ± 1.0 (29)	5.1 ± 1.8 (33)	3.8 ± 1.3 (33)
L, λ	1.4 ± 0.2 (115)	1.4 ± 0.2 (82)	1.3 ± 0.2 (22)	1.4 ± 0.1 (29)	1.4 ± 0.1 (31)	1.3 ± 0.2 (33)
Rheobase, nA	13 ± 7 (113)	12 ± 7 (82)	12 ± 6 (19)	14 ± 7 (32)	10 ± 6 (31)	14 ± 6 (31)
I_{short}, nA	29 ± 14 (77)	28 ± 15 (50)	30 ± 17 (15)	31 ± 14 (23)	20 ± 10 (12)	30 ± 11 (27)
C_{tot}, nF	7.1 ± 1.8 (115)	7.3 ± 1.9 (82)	7.7 ± 2.0 (22)	7.5 ± 1.9 (29)	6.8 ± 1.7 (31)	6.8 ± 1.7 (33)
V_{dep}, mV	11 ± 4 (80)	12 ± 4 (53)	12 ± 4 (16)	12 ± 4 (20)	11 ± 4 (17)	12 ± 4 (27)
V_{thr}, mV	−56 ± 5 (80)	−55 ± 5 (53)	−55 ± 4 (16)	−55 ± 6 (20)	−56 ± 5 (20)	−57 ± 5 (27)
AHP_{dur}, ms	77 ± 26 (96)	78 ± 27 (66)	74 ± 23 (17)	75 ± 24 (27)	86 ± 34 (22)	74 ± 23 (30)
$AHP_{t½}$, ms	21 ± 7 (96)	21 ± 7 (66)	20 ± 6 (17)	20 ± 6 (27)	24 ± 8 (22)	20 ± 6 (30)
AHP_{max}, mV	3.5 ± 1.3 (96)	3.5 ± 1.4 (66)	3.3 ± 1.5 (17)	3.5 ± 1.2 (27)	3.5 ± 1.5 (22)	3.6 ± 1.2 (30)

Values are means + SD. Values in parentheses are number of motoneurons. TS, triceps surae; MG, medial gastrocnemius; LG, lateral gastrocnemius; SOL, soleus; DT, tibial nerve distal to TS nerves; AP, action potential; CV, conduction velocity; R_N, input resistance; τ_m, membrane time constant; L, electrotonic length; rheobase, long current pulse threshold; I_{short}, short current pulse threshold; C_{tot}, whole-cell capacitance; V_{dep}, depolarization from resting potential required for action potential initiation; V_{thr}, absolute threshold voltage for action potential initiation; AHP, afterhyperpolarization; AHP_{dur}, duration of AHP; $AHP_{t½}$, time to half amplitude of AHP; AHP_{max}, maximum amplitude of AHP.

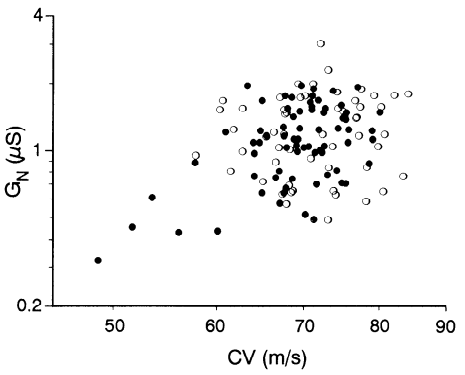

FIG. 2. Log-log relationship between conduction velocity (CV) and input conductance (G_N) for cells with action potentials ≥75 mV (●) and for cells with action potentials ≥60 mV and <75 mV (○).

CV is commonly used as an index of cell size in studies of cat motoneurons because it has a positive linear relationship with soma diameter (Cullheim 1978) and a power relationship with motoneuron surface area (Barrett and Crill 1974; Moschovakis et al. 1991; Ulfhake and Kellerth 1984). Similar relationships are found between CV and soma diameter in a small sample of macaque motoneurons (Lee et al. 1990) and, in the present data, between CV and C_{tot}, which is expected to be proportional to cell surface area [slope 1.2, $r^2 = 0.18$, $P < 0.0001$ for linear regression of log(C_{tot}) on log(CV) for all cells; slope 1.3, $r^2 = 0.26$, $P < 0.0001$ for cells with action potentials ≥75 mV]. These observations support the use of CV as an index (albeit imperfect) of cell size.

Motoneurons with high R_N tend to have low CVs, whereas those with low R_N tend to have high CVs, which is qualitatively similar to the relationship found in cats (Burke 1967, 1968a; Fleshman et al. 1981; Gustafsson and Pinter 1984a; Kernell 1966). Theoretically, input conductance (G_N, the reciprocal of R_N) should be proportional to CV (which is proportional to cell diameter) raised to the power of 1.5–2 for cells with greater to lesser dendritic contribution to G_N (Kernell and Zwaagstra 1981). This simple model assumes that motoneurons of different sizes share common geometric proportions and intrinsic membrane properties. This assumption is likely to be true for these data, because L (and thus the dendritic architecture and intrinsic membrane properties that determine it) does not vary in any consistent way with CV or C_{tot} ($r^2 = 0.00$, $P > 0.6$ for linear regression of L on CV or C_{tot}).

Figure 2 shows the relationship between G_N and CV on double logarithmic axes. Regression analysis indicates a significant relationship between log(CV) and log(G_N) ($r^2 = 0.17$, $P < 0.0001$). Thus, as in cat motoneurons (Burke et al. 1982; Fleshman et al. 1981; Gustafsson and Pinter 1984a), G_N in macaque motoneurons appears to be only modestly dependent on cell size. The slope of the linear regression between these variables (i.e., the power to which the CV is raised to give the best linear fit of the log-transformed data) is 1.8. It should be noted the slope tends to increase as acceptance criteria more restrictive than the standard of action potentials ≥60 mV are applied. For example, the slope of this relationship is 2.2 ($r^2 = 0.26$, $P < 0.0001$) for all cells with action potentials ≥75 mV (Fig. 2, ●). This value appears to approximate the maximum in that the slope does not vary by >10% as the acceptance criterion varies in 1-mV steps between 74 and 82 mV. Thus the slope of this relationship probably falls in the range of 1.8–2.2, which is consistent with the prediction of the simple model described above. In cats, comparable results have been obtained in some studies (Barrett and Crill 1974; Gustafsson and Pinter 1984a), but substantially higher slope values have been reported elsewhere (Kernell and Zwaagstra 1981). The wide range of values across studies may reflect differences in the criteria used for accepting motoneurons into the data pool and/or in the method used to determine R_N (see DISCUSSION).

Although R_m could not be evaluated directly in this study, it is proportional to τ_m, since membrane capacitance (C_m) appears to have a characteristic value for lipid bilayer membranes, varying little among different types of neurons (Rall 1977). R_N varies with τ_m (Fig. 3*A*), with a linear regression accounting for a substantial portion of the variation in R_N ($r^2 = 0.59$, $P < 0.0001$). Because R_m is a common determinant of both variables, these data suggest that R_m varies considerably in macaque motoneurons, as it also appears to do in cat motoneurons (Gustafsson and Pinter 1984a; Ulfhake and Kellerth 1984).

The relationship between τ_m and R_N would be expected to be linear only if the contributions of the other factors (i.e., L and surface area) are constant. L tends to be longer in cells with shorter τ_m and shorter in cells with long τ_m. A significant, but weak, relationship is found between L and $1/\sqrt{\tau_m}$ ($r^2 = 0.16$, $P < 0.0001$) as seen in cat motoneurons, which is consistent with the predicted inverse relationship between L and $\sqrt{R_m}$ (Gustafsson and Pinter 1984a). Be-

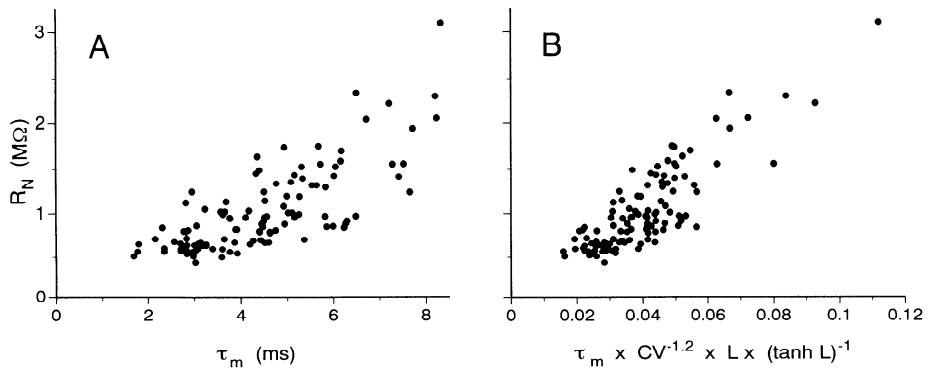

FIG. 3. Relationships between input resistance (R_N) and (*A*) membrane time constant (τ_m) and (*B*) the combination of variables from the right side of *Eq. 1*.

cause L appears to be independent of CV and C_{tot} (see above), factors related to cell size and geometry could contribute independently to R_N. These data indicate that R_N and motoneuron electrophysiological and anatomic properties are related in a complex way.

At present, the extent to which Rall's model of the relationship between R_N and cell size, membrane properties, and geometry is applicable to macaque motoneurons cannot be assessed directly, because there are no detailed anatomic data with which to estimate R_m and to determine whether the underlying assumptions of the model are met. However, assuming that τ_m is proportional to R_m and that CV raised to the power of 1.2 is proportional to motoneuron surface area (see above), the model predicts that

$$R_N \propto \tau_m \times \frac{1}{CV^{1.2}} \times \frac{L}{\tanh L} \qquad (1)$$

Figure 3*B* shows that there is strong linear relationship between R_N and the multiplicative combination of variables on the right side of *Eq. 1* ($r^2 = 0.73$, $P < 0.0001$). This suggests that this model provides a reasonable approximation of the relationship between R_N and these macaque motoneuron properties.

Motoneuron excitability

Rheobase, the current threshold of a neuron, is by definition a measure of excitability. It is expected to be dependent on passive properties related to G_N, action potential threshold properties, and other voltage-dependent properties active between resting and threshold potentials. Figure 4 shows that rheobase varies directly with G_N in macaque motoneurons ($r^2 = 0.34$, $P < 0.0001$ for linear regression; $r^2 = 0.54$, $P < 0.0001$ for cells with action potentials ≥75 mV). Because much of the variation in R_N can be accounted for by factors related to cell morphology and R_m, rheobase would also be expected to vary similarly with these variables. In fact, rheobase varies directly with C_{tot} ($r^2 = 0.18$, $P < 0.0001$ for regression of rheobase on C_{tot}) and inversely with τ_m ($r^2 = 0.10$, $P < 0.001$ for regression of rheobase on $1/\tau_m$). Stronger relationships are evident using more restrictive acceptance criteria (e.g., $r^2 = 0.26$ and 0.25 for cells with action potentials ≥75 mV for regression of

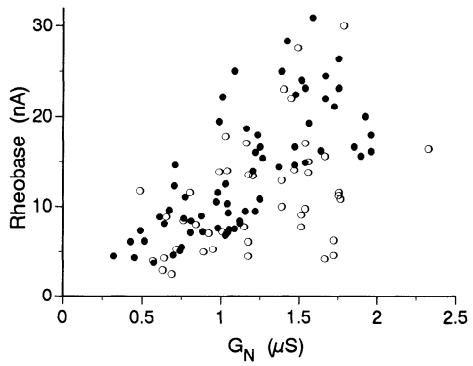

FIG. 4. Relationship between input conductance (G_N) and long current pulse threshold (rheobase) for cells with action potentials >75 mV (●) and for cells with action potentials ≥60 mV and <75 mV (○).

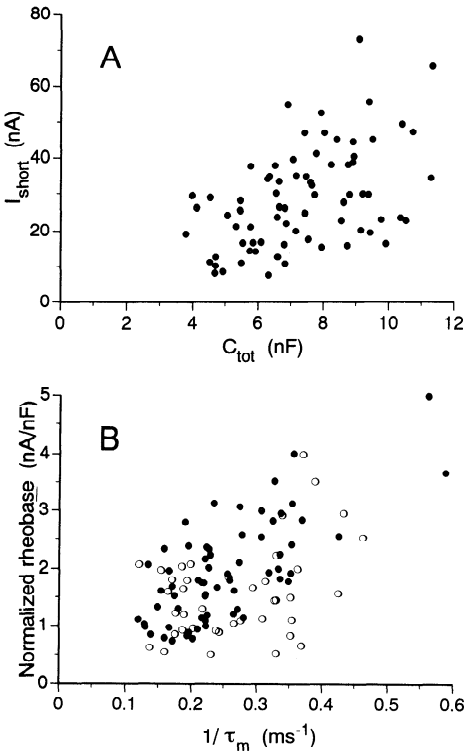

FIG. 5. Relationships between (*A*) whole-cell capacitance (C_{tot}) and short current pulse threshold (I_{short}) for the entire population of cells and (*B*) the inverse of membrane time constant (τ_m) and normalized long current pulse threshold [rheobase (i.e., rheobase/C_{tot})] for cells with action potentials ≥75 mV (●) and for cells with action potentials ≥60 mV and <75 mV (○).

rheobase on C_{tot} and $1/\tau_m$, respectively; $P < 0.0001$ for both regressions).

Because the factors related to cell size, shape, and R_m are themselves interrelated, it difficult to directly assess their relative contributions to rheobase. An alternative approach is to evaluate excitability using I_{short}, which is expected to be determined primarily by cell size and geometry, with resistivity and other factors (e.g., voltage-dependent conductances activated between resting and threshold potentials) having relatively little contribution (Gustafsson and Pinter 1984b). I_{short} varies directly with C_{tot} (Fig. 5*A*; $r^2 = 0.24$, $P < 0.0001$), but does not vary with τ_m ($r^2 = 0.01$, $P > 0.4$ for regression of I_{short} on $1/\tau_m$). Conversely, the role of factors other than cell size can be evaluated by normalizing rheobase by dividing by C_{tot}. To the extent that C_m is constant among motoneurons (Rall 1977), C_{tot} estimates cell surface area, and thus normalized rheobase reflects the cell's current threshold per unit area. That this measure of excitability is independent of cell size is supported by its lack of relationship with CV ($r^2 = 0.01$, $P > 0.2$ for linear regression). Figure 5*B* shows that normalized rheobase is negatively related to τ_m ($r^2 = 0.32$, $P < 0.0001$ for regression of normalized rheobase on $1/\tau_m$; $r^2 = 0.53$, $P < 0.0001$ for cells with action potentials ≥75 mV (●). The relationship is consistent with an inverse relationship between a motoneuron's current threshold per unit area and its R_m. These data suggest that both size and resistivity are determinants of a cell's current threshold, but their relative contri-

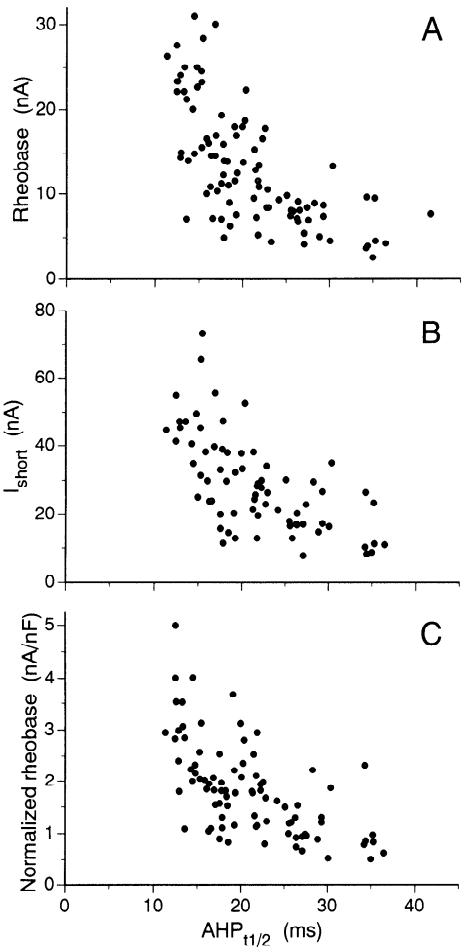

FIG. 6. Relationships between time to half amplitude of the afterhyperpolarization ($AHP_{t½}$) and (*A*) long current pulse threshold (rheobase), (*B*) short current pulse threshold (I_{short}), and (*C*) normalized rheobase [i.e., rheobase/whole-cell capacitance (C_{tot})].

bution depends on the conditions under which the cell is activated.

That the range of G_N predicts a 5-fold range of rheobase values out of the observed 12-fold range suggests that other factors contribute to rheobase. Rheobase is also positively related to V_{dep} ($r^2 = 0.24$, slope 0.76 nA/mV, $P < 0.0001$). On the basis of a model of a purely ohmic, nondendritic cell, V_{dep} is expected to be equivalent to the product of rheobase and R_N (V_{IR}). V_{dep} and V_{IR} are positively related ($r^2 = 0.37$, $P < 0.0001$). However, there is a weak tendency for V_{dep} to be larger than V_{IR} (average within-cell difference 1 ± 4 mV; $0.02 > P > 0.01$). A similar phenomenon observed in cat motoneurons was attributed to the presence of a voltage-dependent process resulting in subthreshold rectification (Gustafsson and Pinter 1984b). However, unlike the situation in cat motoneurons, the difference between V_{dep} and V_{IR} does not appear to vary consistently with AHP_{dur} or τ_m ($r^2 = 0.04$, $P > 0.05$ and $r^2 = 0.00$, $P > 0.7$ for linear regressions, respectively).

In cats, the type of motor unit innervated by a motoneuron appears to be related to the time course of its AHP, and thus it is of interest if this motoneuron property varies in any consistent way with excitability. In the macaque, as in the cat, current thresholds vary systematically with AHP time course. Rheobase, I_{short}, and normalized rheobase are negatively related to $AHP_{t½}$ (Fig. 6, *A–C*, respectively; $r^2 = 0.53$, 0.45, and 0.44 for regression on $1/AHP_{t½}$, respectively, with $P < 0.0001$ for all regressions) and to AHP_{dur} ($r^2 = 0.38$, 0.43, and 0.35, for regression on $1/AHP_{dur}$, respectively; $P < 0.0001$ for all regressions). These relationships appear to result from the covariation of AHP time course measurements with several factors that contribute to determining motoneuron excitability. Multiple regression of rheobase on three factors related to cell size, R_m, and voltage threshold (i.e., C_{tot}, τ_m, and V_{dep}, respectively) accounts for a substantial amount of the variance in rheobase and I_{short} (Table 3). Each of the three independent variables uniquely accounts for a significant portion of the total variation in rheobase or I_{short}. For I_{short}, the r^2 unique to $1/\tau_m$ is small, which is consistent with R_m having little impact on excitability using short current pulses. For both regressions, the sum of the r^2 uniquely attributable to each independent variable approximates the r^2 for the whole regression model, suggesting that each factor contributes independently to excitability. Inclusion of $1/AHP_{t½}$ as a fourth independent variable in the multiple regressions (Table 3) only results in modest increase in whole model r^2, despite the large r^2 obtained using $1/AHP_{t½}$ alone in simple regressions (see above). The r^2 unique to each independent variable decreases such that their sum represents less than half of the r^2 for the whole regression model. These analyses suggest that $AHP_{t½}$ largely accounts for the same aspects of rheobase and I_{short} as do τ_m, C_{tot}, and V_{dep}. Inclusion of membrane potential as an additional factor in the multiple regression analysis does not alter this outcome. Individually, each of these three independent variables are weakly related to $AHP_{t½}$ (Table 4), but together they form a spectrum of motoneuron properties that are well related to $AHP_{t½}$. Thus the systematic covariation of several moto-

TABLE 3. *Regression analysis of dependence of rheobase on C_{tot}, τ_m, V_{dep}, and $AHP_{t½}$*

Dependent Variable	Independent Variable	r^2 Without $AHP_{t½}$	r^2 With $AHP_{t½}$
Rheobase	$1/\tau_m$	0.19*	0.04†
	C_{tot}	0.19*	0.06†
	V_{dep}	0.19*	0.10*
	$1/AHP_{t½}$	NA	0.10*
Sum of r^2		0.57	0.30
Whole model r^2		0.57*	0.71*
I_{short}	$1/\tau_m$	0.05†	0.00
	C_{tot}	0.15*	0.03
	V_{dep}	0.42*	0.24*
	$1/AHP_{t½}$	NA	0.10*
Sum of r^2		0.62	0.37
Whole model r^2		0.67*	0.78*

For each independent variable in the multiple regressions, r^2 is the variance accounted for by the variable alone, sum of r^2 is the algebraic sum of the individual r^2 values, and whole model r^2 is the variance accounted for by regression on all independent variables. Abbreviations, see Table 2. NA, not applicable. *$P < 0.0001$. †$P < 0.01$.

TABLE 4. *Relationships between $AHP_{t½}$ and other motoneuron properties*

Independent variable	Slope	Intercept	r^2	n
τ_m*	1.54	14.8	0.09	90
C_{tot}*	−1.16	29.4	0.10	89
CV*	−0.44	52.1	0.14	96
L	−8.91	33.1	0.05	89
V_{dep}†	−0.47	26.6	0.09	71
V_{thr}	−0.20	9.78	0.03	71
R_N‡	10.5	11.4	0.28	89

Abbreviations, see Table 2. *$P < 0.01$. †$P = 0.01$. ‡$P < 0.0001$ for regression of $AHP_{t½}$ on motoneuron property.

neuron properties related to excitability may contribute to the pattern of recruitment.

Both rheobase and V_{dep} tend to be lower in cells with more depolarized resting membrane potentials ($r^2 = 0.09$, $P < 0.01$ and $r^2 = 0.19$, $P < 0.0001$, respectively, for regressions on resting potential), although V_{dep} decreases more gradually than the resting potential rises (slope of regression line −0.30 mV/mV). This probably reflects the tendency of V_{thr} to be less negative for more depolarized resting potentials ($r^2 = 0.51$, $P < 0.0001$ for linear regression). Similar variation in V_{thr} with resting potential has been reported for cat motoneurons (Pinter et al. 1983) and could reflect the voltage dependence of the mechanism responsible for action potential initiation.

Although a large portion of the variation in V_{thr} can be accounted for by variations in resting potential, differences in motoneuron excitability could result from systematic variations in V_{thr} with other factors. As reported for cat motoneurons (Pinter et al. 1983), V_{thr} is not differentially distributed among motoneuron pools (Table 2) and is not significantly related to CV, AHP_{dur}, $AHP_{t½}$, R_N, or L in a way that is independent of resting potential ($P > 0.1$ for unique contribution of each property to multiple regression of V_{thr} on resting potential and each property). However, V_{thr} is positively, but weakly, related to C_{tot} in way that is independent of resting potential ($r^2 = 0.06$, $P < 0.01$ for unique contribution of C_{tot} to multiple regression of V_{thr} on resting potential and C_{tot}). Although the tendency of V_{thr} to be more depolarized in larger cells could contribute to the preferential recruitment of smaller motoneurons, the weakness of the relationship between V_{thr} and C_{tot} suggests that this mechanism is not a major determinant of recruitment order in macaque motoneurons.

DISCUSSION

Interspecies differences in motoneuron properties

Most studies of spinal motoneuron properties have been performed in cats, whereas relatively few have evaluated these properties in primates. Table 5 presents data on primate TS motoneurons from the present study and from another primate study and those from cat studies. The differences seen between cat and macaque are likely to reflect differences in intrinsic properties between macaque and cat motoneurons.

τ_m appears to be shorter and R_N appears to be lower in macaque TS motoneurons than in cat TS motoneurons. In the present study, as in cat (Burke 1968a), SOL motoneurons tend to have longer τ_m and higher R_N than gastrocnemius motoneurons. Thus an artifactual interspecies difference in these properties could occur if the present study consisted of a lower proportion of SOL cells than the cat studies. For the cat study in Table 5 in which the motoneuron distribution is available (Burke 1968a), the TS data sample consisted of 17% SOL motoneurons, whereas that in the present study consisted of 36% SOL motoneurons. This would tend to bias the present data toward higher average values for τ_m and R_N in TS motoneurons, suggesting that the interspecies differences in these properties cannot be attributed simply to differential sampling of TS motoneurons. Thus the differences in τ_m and R_N most likely reflect differences in motoneuron properties between cat and macaque. Assuming that C_m does not vary systematically among motoneurons (Rall 1977), the shorter values of τ_m in macaque suggest that R_m is lower than in cat. The comparably lower values of R_N in macaque are consistent with lower values of R_m in this species, because R_m is an important determinant of R_N.

Another interspecies difference is that CV of macaque TS motoneurons is lower than that of cat TS motoneurons. This difference is unlikely to be due to sampling bias resulting from a high percentage of SOL motoneurons in the present study, because the CVs of both SOL and gastrocnemius motoneurons are lower in macaque than cat (Burke 1967). In addition, the average CV of macaque TS motoneurons is similar to that of baboon TS motoneurons

TABLE 5. *Comparison of TS motoneuron properties among studies in cats and primates*

	Cat		Baboon	Macaque
	Burke 1967, 1968a	Gustafsson and Pinter 1984a,b	Hongo et al. 1984	Present study
CV, m/s	99 ± 2 (72–125)	83 ± 1 (51–110)	68 ± 1 (57–76)	71 ± 1 (49–87)
R_N, MΩ	1.3 ± 0.1 (0.4–5.9)	1.5 ± 0.1 (0.6–4.0)		1.0 ± 0.1 (0.3–3.1)
τ_m, ms	5.5 ± 0.3 (2.8–9.3)	4.9 ± 0.3 (2.1–9.1)		4.6 ± 0.2 (1.8–8.3)
AHP_{dur}, ms	66 ± 3 (25–135)	77 ± 4 (39–150)	82 ± 4 (52–117)	78 ± 3 (42–157)
C_{tot}, nF		6.1 ± 0.2 (2.4–8.4)		7.3 ± 0.2 (3.9–11.3)
Rheobase, nA		13 ± 1 (1–29)		12 ± 1 (3–31)

Values are means ± SE. Values in parentheses are ranges. In studies where values were not reported in the text, estimates were obtained from scatter plots using a high-resolution digitizing pad or from histograms. Data are pooled for all three TS muscles. Abbreviations, see Table 2.

(Hongo et al. 1984) and other nonhuman primate spinal motoneurons (Clough et al. 1968b; Gilliatt et al. 1976; McLeod and Wray 1967). The CV of human motoneurons is even slower than that of nonhuman primates (Borg et al. 1978; Dengler and Stein 1987; Smorto and Basmajian 1979).

The differences in CV among these species do not appear to be related to differences in axon size, because axon diameter (and its correlate, soma diameter) are comparable among cats (Boyd and Davey 1968; Cullheim 1978), nonhuman primates (Janjua and Leong 1987; Jenny and Inukai 1983; Lee et al. 1990; C. L. Lee and J. R. Wolpaw, unpublished data), and humans (Kawamura et al. 1977). Similarly, the interspecies difference in CV is unlikely to result from a difference in the proportion of myelin to axon in the fiber, because large-diameter myelinated axons in cat (Arbuthnott et al. 1980) and human (Schroder et al. 1988) compose ~60–75% of total fiber diameter, a range within which variations in this proportion are expected to have little effect on CV (Goldman and Albus 1968; Smith and Koles 1970). Thus the large interspecies difference in CV is probably due to other factors, such as myelin sheath resistance, internodal distance, or intrinsic properties of the axonal membrane (Coppin and Jack 1971; Friede 1986; Funch and Faber 1984; Moore et al. 1978). For example, a lower value of R_m in primates than in cats, as suggested above for the present data, could contribute to the interspecies difference in CV, assuming that differences in somatodendritic R_m are also present in the axonal membrane.

Interspecies differences in distributions of motoneuron properties between motoneuron pools

The distributions of CV, AHP_{dur}, and R_N between motoneurons innervating gastrocnemius and SOL muscles appear to be less pronounced in macaque than in cat. In macaque, the average CV of gastrocnemius motoneurons is 7% higher than that of SOL motoneurons, whereas it is 20–24% higher in cat; in macaque, AHP_{dur} is only 15% longer in SOL and than in gastrocnemius, whereas in cat, it is 58–79% longer in SOL than in gastrocnemius; and in macaque, the average R_N is 33% higher in SOL than in gastrocnemius, whereas in cat, it is 82–180% higher in SOL than in gastrocnemius [cat data from Burke (1967), Burke et al. (1982), Cullheim (1978), and Hammarberg and Kellerth (1975)].

These differences could result from the differential distribution between macaque and cat of some common factor with which each of these properties covaries. One possible factor is motor unit type. In cat, the distribution of motor unit types differs in gastrocnemius and SOL muscle. Cat SOL muscle consists of ~95–100% slow twitch fibers, whereas gastrocnemius muscles are composed of only ~25% slow-twitch fibers (Burke 1981). Motoneurons innervating S-type motor units tend to be smaller and to have higher R_N and longer AHP time courses than those innervating F-type motoneurons (Burke 1967, 1968a; Burke and ten Bruggencate 1971; Burke et al. 1982; Hammarberg and Kellerth 1975; Ulfhake and Kellerth 1982). On the basis of the distribution of motor unit types in these two muscles, cat SOL motoneurons would be expected to have, on average, lower CV, higher R_N, and longer AHP time course than gastrocnemius motoneurons. Thus, if the distributions of motor unit types in macaque gastrocnemius and SOL were more similar than in cat, the observed similarities in CV, AHP_{dur}, and R_N of gastrocnemius and SOL of macaque would be expected.

The fiber content of TS muscles in *Macaca nemestrina* is unknown, and other primates display considerable diversity in distribution of motor unit types. For example, the distribution of fiber types in TS muscles of cats is comparable to that of another nonhuman primate (*Cynomolgus*), in which ~94% of SOL muscle fibers and only 23% of gastrocnemius muscle fibers have slow-oxidative characteristics (Acosta and Roy 1987). In contrast, in human, the distribution of TS fiber types is more symmetric, in that 71–80% of SOL motor units and 51–64% of gastrocnemius motor units are slow-twitch (Saltin and Gollnick 1983). The present data (i.e., the relatively small differences in motoneuron properties between gastrocnemius and SOL) are consistent with a more homogeneous (i.e., humanlike) distribution of motor unit types among TS muscles in *Macaca nemestrina* than in cats. However, in the absence of direct information on the distribution of macaque motor unit types and the relationships between motoneuron properties and motor unit type, inferences drawn from the present data concerning this issue must be regarded as tentative.

Relationships between motoneuron properties in macaque and cat

Although the absolute values of CV, R_N and τ_m appear to be lower in macaque than in cat, the relationships between motoneuron properties in these species are generally comparable. For example, R_N appears to depend on R_m, and to a lesser extent on cell size and shape. The complex interaction of these factors described by Rall's model of a neuron's electrotonic behavior appears to account for a substantial part of the variation in R_N in macaque. Because this model is also applicable (with some limitations) to cat motoneurons (Barrett and Crill 1974; Burke and ten Bruggencate 1971; Burke et al. 1982; Fleshman et al. 1988; Gustafsson and Pinter 1984a; Ulfhake and Kellerth 1984), the relationships between motoneuron geometry and intrinsic membrane properties would appear to be similar in these species. Similarly, motoneuron excitability in both cats and macaques is related to variables that are expected to reflect R_m, cell size and shape, and action potential threshold properties. The relative importance of these factors depends on the form of the depolarizing input.

The present primate data are consistent with the hypothesis that systematic variations in motoneuron properties contribute to the establishment of stereotypic recruitment of motoneurons (Gustafsson and Pinter 1985a; Zucker 1973). However, the relative contributions of these properties differs between cat and macaque. In cats, F- and S-type motor units can be distinguished by $AHP_{t½}$ (Zengel et al. 1985),[1] a property that also varies with motoneuron excit-

[1] The data of Zengel et al. (1985) indicate that $AHP_{t½}$ can predict correctly whether motoneurons innervate F-type or S-type motor units in 145 out of 148 cases (98%). However, $AHP_{t½}$ does not distinguish among specific F-type motor units [i.e., FF, FI, and FR (Burke, 1981)], because the ranges of this motoneuron property for these motor unit types are almost identical.

ability. In this species, AHP time course is much more closely related to τ_m than to motoneuron size-related properties (Gustafsson and Pinter 1984a), and R_m appears to be higher in S- than in F-type motor units (Burke et al. 1982). Thus R_m is probably not randomly distributed among cat motoneurons, but varies systematically with motor unit type in a size-independent manner. In macaque, motoneuron excitability also varies with $AHP_{t½}$. However, this relationship does not appear to result from a (presumably) type-dependent variation in any one motoneuron property. Rather, it appears to reflect the covariation of several properties that are related to motoneuron size, R_m, and voltage threshold. Although the factors underlying the distribution of motoneuron excitability appear to differ between cat and macaque, the data suggest that the distributions of intrinsic motoneuron properties in the two species probably contribute to qualitatively similar patterns of motoneuron recruitment.

The present primate data do not support any significant variation of R_m strictly on the basis of motoneuron size. The slope of the relationship between log(CV) and log(G_N) conforms to values that are predicted by the assumption that large motoneurons are simply scaled-up versions of small motoneurons with no systematic variation in R_m with motoneuron size. These observations are consistent with studies combining anatomic and electrophysiological data from cat motoneurons that provide little support for any relationship between R_m and motoneuron surface area or soma diameter (Barrett and Crill 1974; Lux et al. 1970; Ulfhake and Kellerth 1984). This slope value for macaque motoneurons is comparable to data from some (Barrett and Crill 1974; Gustafsson and Pinter 1984a) but not all (Burke 1967; Kernell and Zwaagstra 1981) cat studies (summarized in Table 6). The higher-than-expected slope values reported in one of the latter studies (Kernell and Zwaagstra 1981) could not be accounted for on the basis of anatomic differences among motoneurons of different size, which led to the hypothesis that higher-CV motoneurons have lower R_m than lower-CV motoneurons.

TABLE 6. *Comparison among studies of slope of linear regression of log (G_N) on log (CV)*

	Slope		
	Mixed	TS	Method
Present data			$\Delta V/\Delta I$
Cells with action potentials ≥60 mV	1.8	1.9	
Cells with action potentials ≥75 mV	2.2	2.3	
Barrett and Crill (1974)	1.8		$\Delta V/\Delta I$
Gustafsson and Pinter (1984a)	1.9	1.9	$\Delta V/\Delta I$
Burke (1968b)		2.5	Spike-height
Burke (1967)		3.0	Spike-height
Kernell and Zwaagstra (1981)	3.6	2.9	Spike-height
Kernell (1966)	4.0	4.2	Spike-height

Slopes are given for data from motoneurons innervating TS muscles or heterogeneous hindlimb muscles including TS (mixed). Slopes for data from Burke (1967) and Kernell (1966) were reported in Kernell and Zwaagstra (1981). The slope for data from Barrett and Crill (1974) was calculated from data reported in their Table 1. The slope for data from Burke (1968b) was calculated using estimates of data points from their Fig. 6 made with a high-resolution digitizing pad. The two methods used for determining R_N (spike-height and $\Delta V/\Delta I$) are described in the text. All studies were performed in pentobarbital-anesthetized animals, except for one performed in decerebrate cats (Burke 1968b). Abbreviations, see Table 2.

The commonly used methods for determining R_N are susceptible to underestimating R_N in motoneurons in which the sag phenomenon (see METHODS) is present (Burke and ten Bruggencate 1971; Gustafsson and Pinter 1984a; Ito and Oshima 1965). The membrane potential sag is more prominent in F-type motoneurons in cat (Zengel et al. 1985) and in motoneurons with shorter AHP time courses in macaque (see METHODS) and in cat (Gustafsson and Pinter 1984a). Because these motoneurons tend to have higher CVs (Table 4; Ulfhake and Kellerth 1984; Zwaagstra and Kernell 1980), the underestimation of R_N in these motoneurons is likely to be more pronounced than in those with lower CVs and thereby cause the slope of the relationship between log(CV) and log(G_N) to be overestimated. The magnitude of this error would be expected to be dependent (at least in part) on the relationship between the time after current pulse onset at which R_N is calculated and the time course of the sag. In studies where R_N was estimated from the amplitude of a small current pulse and the amplitude of the induced membrane potential change ($\Delta V/\Delta I$ method), the time to peak voltage is expected to be short relative to the apparent τ_{sag} [e.g., in the present study, mean time to peak and $\tau_{sag} \pm SD = 14 \pm 6$ and 49 ± 15 ms, respectively, which is consistent with the small sag-induced underestimation of R_N (see METHODS)]. In contrast, in studies where R_N is estimated from the slope of the relationship between the amplitude of antidromically activated action potentials and current pulse amplitude during which the action potential is elicited (spike-height method), the magnitude of sag-induced error should depend on the relationship between the time to action potential onset and τ_{sag}. For example, Kernell and Zwaagstra (1981) elicited action potentials ~450 ms after the onset of the current pulse, at which time the contribution of the sag process to total membrane conductance is likely to be almost fully developed. The high slope value obtained in this study is consistent with a greater degree of systematic underestimation of R_N in higher CV motoneurons than in studies using the $\Delta V/\Delta I$ method. Studies using the spike-height method with shorter (30–40 ms) current pulses (Burke 1967, 1968b) obtained intermediate slope values. Thus estimates of the slope of the relationship between log(CV) and log(G_N) are probably more reliable when G_N is estimated at a time that is shorter than τ_{sag} (e.g., those using the $\Delta V/\Delta I$ method or those using the spike-height method with short current pulses in Table 6).

In summary, the data reveal that relationships between motoneuron properties reflecting size, passive membrane properties, and voltage threshold are in general similar in cat and macaque. To the extent that these properties determine excitability, motor unit recruitment should also be similar in the two species. At the same time, cat and macaque differ in the distributions of motoneuron properties between the individual TS muscles. These differences may be secondary to difference in distributions of motor unit types. Understanding of the origin and significance of these

distributional differences in motoneuron properties awaits knowledge of TS muscle composition and function in macaque and further evaluation of the relationships between motoneuron properties and motor unit type.

The author thanks Dr. J. R. Wolpaw for technical assistance and for critical review of this manuscript. The author also thanks Mr. A. Herchenroder, who designed and constructed essential mechanical devices used in these experiments, and P. A. Herchenroder, D. M. Maniccia, L. Becker, T. Jarrell, and K. L. Hurley for their expert technical assistance. The author also thanks Dr. C. L. Lee for technical contributions and participation in the early experiments of this study and Drs. C. J. Heckman, R. K. Powers, and D. J. McFarland for their critical review of this manuscript.

This work was supported in part by National Institute of Neurological and Communicative Disorders and Stroke Grant NS-22189 and by a grant from the Paralyzed Veterans of America Spinal Cord Research Foundation.

Address for reprint requests: CNS Studies Section, Wadsworth Center for Laboratories and Research, New York State Dept. of Health, PO Box 509, Albany, NY 12201-0509.

Received 24 October 1991; accepted in final form 26 May 1992.

REFERENCES

ACOSTA, L. AND ROY, R. R. Fiber-type composition of selected hindlimb muscles of a primate (Cynomolgus monkey). *Anat. Rec.* 218: 136–141, 1987.

ARBUTHNOTT, E. R., BOYD, I. A., AND KALU, K. U. Ultrastructural dimensions of myelinated peripheral nerve fibers in the cat and their relation to conduction velocity. *J. Physiol. Lond.* 308: 125–157, 1980.

ASHBY, P. AND ZILM, D. Characteristics of postsynaptic potentials produced in single human motoneurons by homonymous group I volleys. *Exp. Brain Res.* 47: 41–48, 1982.

BALDISSERA, F., HULTBORN, H., AND ILLERT, M. Integration in spinal neuronal systems. In: *Handbook of Physiology. The Nervous System. Motor Control.* Bethesda, MD: Am. Physiol. Soc., 1981, sect. 1, vol. II, part 1, p. 509–595.

BARRETT, J. N. AND CRILL, W. E. Specific membrane properties of cat motoneurons. *J. Physiol. Lond.* 239: 301–324, 1974.

BERGMANS, J., DELWAIDE, P. J., AND GADEA-CIRIA, M. Short-latency effects of low-threshold muscular afferent fibers on different motoneuronal pools of the lower limb in man. *Exp. Neurol.* 60: 380–385, 1978.

BORG, J., GRIMBY, L., AND HANNERZ, J. Axonal conduction velocity and voluntary discharge properties of individual short toe extensor motor units in man. *J. Physiol. Lond.* 277: 143–152, 1978.

BOYD, I. A. AND DAVEY, M. R. *Composition of Peripheral Nerves.* London, Livingstone, 1968.

BURKE, R. E. Motor unit types of cat triceps surae muscle. *J. Physiol. Lond.* 193: 141–160, 1967.

BURKE, R. E. Group Ia synaptic input to fast and slow twitch motor units of cat triceps surae. *J. Physiol. Lond.* 196: 605–630, 1968a.

BURKE, R. E. Firing patterns of gastrocnemius motor units in the decerebrate cat. *J. Physiol. Lond.* 196: 631–654, 1968b.

BURKE, R. E. Motor units: anatomy, physiology, and functional organization. In: *Handbook of Physiology. The Nervous System. Motor Control.* Bethesda, MD: Am. Physiol. Soc., 1981, sect. 1, vol. II, part 1, p. 345–422.

BURKE, R. E., DUM, R. P., FLESHMAN, J. W., GLENN, L. L., LEV TOV, A., O'DONOVAN, M. J., AND PINTER, M. J. A HRP study of the relation between cell size and motor unit type in cat ankle extensor motoneurons. *J. Comp. Neurol.* 209: 17–28, 1982.

BURKE, R. E. AND TEN BRUGGENCATE, G. Electrotonic characteristics of alpha motoneurones of varying size. *J. Physiol. Lond.* 212: 1–20, 1971.

CARP, J. S., LEE, C. L., AND WOLPAW, J. R. Physiologic properties of primate lumbar motoneurons: initial studies. *Soc. Neurosci. Abstr.* 15: 697, 1989.

CARP, J. S. AND WOLPAW, J. R. Motoneuron physiology after H-reflex operant conditioning: initial studies. *Soc. Neurosci. Abstr.* 16: 115, 1990.

CLOUGH, J. F. M., KERNELL, D., AND PHILLIPS, C. G. The distribution of monosynaptic excitation from the pyramidal tract and from primary spindle afferents to motoneurones of the baboon's hand and forearm. *J. Physiol. Lond.* 198: 145–166, 1968a.

CLOUGH, J. F. M., KERNELL, D., AND PHILLIPS, C. G. Conduction velocity in proximal and distal portions of forelimb axons in the baboon. *J. Physiol. Lond.* 198: 167–178, 1968b.

COPPIN, C. M. L. AND JACK, J. J. B. Internodal length and conduction velocity of cat muscle afferent nerve fibers. *J. Physiol. Lond.* 22: 91–93, 1971.

CULLHEIM, S. Relations between cell body size, axon diameter and axon conduction velocity of cat sciatic alpha-motoneurons stained with horseradish peroxidase. *Neurosci. Lett.* 8: 17–20, 1978.

DENGLER, R. AND STEIN, R. B. Direckte Messung der Leitgeschwindigkeit einzelner motorischer Axone am Menschen. *Z. EEG-EMG* 18: 68–71, 1987.

DOLD, G. M. AND BURKE, R. E. A joystick operated microforge for fabrication of glass micropipette electrodes. *Electroencephalogr. Clin. Neurophysiol.* 33: 232–235, 1972.

ECCLES, J. C., ECCLES, R. M., AND LUNDBERG, A. The convergence of monosynaptic excitatory afferents onto many different species of alpha motoneurons. *J. Physiol. Lond.* 137: 22–50, 1957.

FLESHMAN, J. W., MUNSON, J. B., SYPERT, G. W., AND FRIEDMAN, W. A. Rheobase, input resistance, and motor-unit type in medial gastrocnemius motoneurons in the cat. *J. Neurophysiol.* 46: 1326–1338, 1981.

FLESHMAN, J. W., SEGEV, I., AND BURKE, R. E. Electrotonic architecture of type-identified alpha-motoneurons in the cat spinal cord. *J. Neurophysiol.* 60: 60–85, 1988.

FRIEDE, R. L. Relation between myelin sheath thickness, internode geometry, and sheath resistance. *Exp. Neurol.* 92: 234–247, 1986.

FUNCH, P. G. AND FABER, D. S. Measurement of myelin sheath resistances: implications for axonal conduction and pathology. *Science Wash. DC* 225: 538–540, 1984.

GILLIATT, R. W., HOPF, H. C., RUDGE, P., AND BARAITSER, M. Axonal velocities of motor units in the hand and foot muscles of the baboon. *J. Neurol. Sci.* 29: 249–258, 1976.

GOLDMAN, L. AND ALBUS, J. S. Computation of impulse conduction in myelinated fibres: theoretical basis of the velocity-diameter relation. *Biophys. J.* 8: 596–607, 1968.

GREEN, C. J. *Animal Anesthesia.* London, Lab. Anim., 1979, p. 217–226.

GUSTAFSSON, B. AND PINTER, M. J. Relations among passive electrical properties of lumbar alpha-motoneurones of the cat. *J. Physiol. Lond.* 356: 401–431, 1984a.

GUSTAFSSON, B. AND PINTER, M. J. An investigation of threshold properties among cat spinal alpha-motoneurones. *J. Physiol. Lond.* 357: 453–483, 1984b.

GUSTAFSSON, B. AND PINTER, M. J. On the factors determining orderly recruitment of motor units: a role for intrinsic membrane properties. *Trends Neurosci.* 8: 431–433, 1985a.

GUSTAFSSON, B. AND PINTER, M. J. Factors determining the variation of the afterhyperpolarization duration in cat lumbar alpha-motoneurons. *Brain Res.* 326: 392–395, 1985b.

HAMMARBERG, C. AND KELLERTH, J.-O. Studies of some twitch and fatigue properties of different motor unit types in the ankle muscles of the adult cat. *Acta Physiol. Scand.* 95: 231–242, 1975.

HONGO, T., LUNDBERG, C. G., PHILLIPS, F. R. S., AND THOMPSON, R. F. The pattern of monosynaptic Ia-connections to hindlimb motor nuclei in the baboon: a comparison with the cat. *Proc. R. Soc. Lond. Ser. B Biol. Sci.* 221: 261–289, 1984.

ITO, M. AND OSHIMA, T. Electrical behaviour of the motoneurone membrane during intracellularly applied current steps. *J. Neurophysiol.* 180: 607–637, 1965.

JACK, J. An introduction to linear cable theory. In: *The Neurosciences Fourth Study Program,* edited by F. Schmitt and F. G. Worden. Cambridge, MA: MIT Press, 1979, p. 423–437.

JANJUA, M. Z. AND LEONG, S. K. Sensory, motor and sympathetic neurons forming the common peroneal and tibial nerves in the macaque monkey (*Macaca fascicularis*). *J. Anat.* 153: 63–76, 1987.

JENNY, A. B. AND INUKAI, J. Principles of motor organization of the monkey cervical spinal cord. *J. Neurosci.* 3: 567–575, 1983.

KAWAMURA, Y., O'BRIEN, P., OKAZAKI, H., AND DYCK, P. J. Lumbar motoneurons of man. II. The number and diameter distribution of large- and intermediate- diameter cytons in "motoneuron columns" of spinal cord of man. *J. Neuropathol. Exp. Neurol.* 36: 861–870, 1977.

KERNELL, D. Input resistance, electrical excitability, and size of ventral horn cells in cat spinal cord. *Science Wash. DC* 152: 1637–1640, 1966.

KERNELL, D. AND ZWAAGSTRA, B. Input resistance, axonal conduction velocity and cell size among hindlimb motoneurones of the cat. *Brain Res.* 204: 311–326, 1981.

LEE, C. L., CARP, J. S., AND WOLPAW, J. R. Triceps surae motoneurons and Ia afferent connections: further anatomical studies. *Soc. Neurosci. Abstr.* 16: 115, 1990.

LUX, H. D., SCHUBERT, P., AND KREUTZBERG, G. W. Direct matching of morphological and electrophysiological data in cat spinal motoneurons. In: *Excitatory Synaptic Mechanisms,* edited by P. Anderson and J. K. S. Jansen. Oslo: Universitetsforlaget, 1970, p. 189–198.

MAO, C. C., ASHBY, P., WANG, M., AND MCCREA, D. Synaptic connections from large muscle afferents to the motoneurons of various leg muscles in man. *Exp. Brain Res.* 56: 341–350, 1984.

MCLEOD, J. G. AND WRAY, S. H. Conduction velocity and fibre diameter of the median and ulnar nerves of the baboon. *J. Neurol. Neurosurg. Psychiatry* 30: 240–247, 1967.

MOORE, J. W., JOYNER, R. W., BRILL, M. H., WAXMAN, S. D., AND NAJAR-JOA, M. Simulations of conduction in uniform myelinated fibers: relative sensitivity to changes in nodal and internodal parameters. *Biophys. J.* 21: 147–160, 1978.

MOSCHOVAKIS, A. K., BURKE, R. E., AND FYFFE, R. E. W. The size and dendritic structure of HRP-labeled gamma motoneurons in the cat spinal cord. *J. Comp. Neurol.* 311: 531–545, 1991.

PIERROT-DESEILLIGNY, E., MORIN, C., BERGEGO, C., AND TANKOV, N. Pattern of group I fibre projections from ankle flexor and extensor muscles in man. *Exp. Brain Res.* 42: 337–350, 1981.

PINTER, M. J., CURTIS, R. L., AND HOSKO, M. J. Voltage threshold and excitability among variously sized cat hindlimb motoneurons. *J. Neurophysiol.* 50: 644–657, 1983.

RALL, W. Time constants and electrotonic length of membrane cylinders and neurons. *Biophys. J.* 9: 1483–1508, 1969.

RALL, W. Core conductor theory and cable properties of neurons. In: *Handbook of Physiology. The Nervous System. Cellular Biology of Neurons.* Bethesda, MD: Am. Physiol. Soc., 1977, sect. 1, vol. I, p. 39–97.

ROSE, P. K. AND VANNER, S. J. Differences in somatic and dendritic specific membrane resistivity of spinal motoneurons: an electrophysiological study of neck and shoulder motoneurons in the cat. *J. Neurophysiol.* 60: 149–166, 1988.

SALTIN, B. AND GOLLNICK, P. D. Skeletal muscle adaptability: significance for metabolism and performance. In: *Handbook of Physiology. Skeletal Muscle.* Bethesda, MD: Am. Physiol. Soc., 1983, sect. 10, p. 555–631.

SCHRODER, J. M., BOHL, J., AND VON BARDELEBEN, U. Changes of the ratio between myelin thickness and axon diameter in human developing sural, ulnar, facial and trochlear nerves. *Acta Neuropathol.* 76: 471–483, 1988.

SMITH, R. S. AND KOLES, Z. J. Myelinated nerve fibers: computed effect of myelin thickness on conduction velocity. *Am. J. Physiol.* 219: 1256–1258, 1970.

SMORTO, M. P. AND BASMAJIAN, J. V. *Clinical Electroneurography: An Introduction to Nerve Conduction Tests.* Baltimore, MD: Williams and Wilkins, 1979.

STEFFEY, E. P. Concepts of general anesthesia and assessment of adequacy of anesthesia for animal surgery. In: *Animal Pain: Perception and Alleviation,* edited by R. L. Kitchell, H. H. Erickson, E. Carstens, and L. E. Davis. Bethesda, MD: Am. Physiol. Soc., 1983, p. 133–150.

ULFHAKE, B. AND KELLERTH, J.-O. Does alpha-motoneurone size correlate with motor unit type in cat triceps surae? *Brain Res.* 251: 201–209, 1982.

ULFHAKE, B. AND KELLERTH, J.-O. Electrophysiological and morphological measurements in cat gastrocnemius and soleus alpha-motoneurones. *Brain Res.* 307: 167–179, 1984.

WOLPAW, J. R. Operant conditioning of primate spinal reflexes: the H-reflex. *J. Neurophysiol.* 57: 443–458, 1987.

WOLPAW, J. R. AND LEE, C. L. Memory traces in primate spinal cord produced by operant conditioning of H-reflex. *J. Neurophysiol.* 61: 563–572, 1989.

ZENGEL, J. E., REID, S. A., SYPERT, G. W., AND MUNSON, J. B. Membrane electric properties and prediction of motor-unit type of medial gastrocnemius motoneurons in the cat. *J. Neurophysiol.* 53: 1323–1344, 1985.

ZUCKER, R. S. Theoretical implications of the size principle of motoneurone recruitment. *J. Theor. Biol.* 38: 587–596, 1973.

ZWAAGSTRA, B. AND KERNELL, D. The duration of after-hyperpolarization in hindlimb alpha motoneurons of different sizes in the cat. *Neurosci. Lett.* 19: 303–307, 1980.